J. Fluid Mech. (1981), *vol.* 107, *pp.* 109–129
Printed in Great Britain

Existence of viscous eddies near boundaries

By N. LIRON
Department of Mathematics, I.I.T. The Technion, Haifa, Israel

AND J. R. BLAKE
Department of Mathematics, The University of Wollongong, P.O. Box 1144, Wollongong, N.S.W. 2500, Australia

(Received 17 December 1979)

Kinematic and dynamic conditions for the existence, or otherwise, of viscous eddies due to point, ring or a line distribution of *stokeslets* near no-slip boundaries are investigated. Boundaries considered are (i) a single plane boundary, (ii) two parallel plane boundaries, (iii) an infinite cylinder, and (iv) a finite cylinder. It is found that the following constraints on the fluid lead to the existence of eddies (i) a zero flux condition, (ii) confinement due to boundaries, (iii) streamline convergence near the singularity, and (iv) the interaction of flow fields due to adjacent stokeslets. The existence or non-existence of various viscous eddies is illustrated and discussed in detail for the case of infinite line distributions of stokeslets (i.e. a two-dimensional stokeslet). The paper suggests that flow fields produced by sessile micro-organisms are determined primarily by the container geometry in which they are located.

1. Introduction

Recent theoretical studies on flows at low Reynolds number in bounded geometries have revealed the existence of viscous eddies of varying shapes and sizes. Moffatt (1964), Liron & Mochon (1976), Davis & O'Neill (1977), Yoo & Joseph (1978), Liu & Joseph (1978) and Blake (1979) have predicted the existence of from one to infinitely many viscous eddies. Except for the works of Liron & Mochon and Blake, these flow fields are produced by some exterior pressure or primary flow field. In all of these studies no attempt was made to isolate the important mechanisms that determine the existence of viscous eddies. Recently Jeffrey & Sherwood (1980) have surveyed the different streamline patterns and eddies that can exist in two-dimensional Stokes flows. They present streamline patterns near stagnation points, and later concentrate their discussion on eddies in corner-like regions. They suggest that the eddies one calculates are a result of two competing components. One is the result of the primary outside flow field stirring the flow, and the other is the modification caused by the local special conditions. In this paper we investigate the basic dynamic and kinematic conditions that determine the size and number of viscous eddies that are produced next to simple geometries. To this end we investigate the formation of (mainly three-dimensional) eddies in different geometries relative to the direction of a point force, or a line distribution of point forces. The reason for choosing point forces to study viscous eddy formation is twofold. Firstly, it enables us to study in isolation the conditions determining the size and number of eddies without additional effects of

external fields. Secondly, such eddies have been observed experimentally in research on sessile micro-organisms with actively beating cilia (or flagella) where the action of the cilia can be represented as a distribution of force singularities.

In a detailed experimental study of the food collection by *Vorticella*, Sleigh & Barlow (1976) not only considered the flow fields around the peristome and infundibulum, but also recorded details of the fluid motion in the far field well away from the body. The particle path lines they observed were almost circular in planes parallel to the slide and coverslip, suggesting that the flow field produced by *Vorticella* has similar streamlines to that produced by a two-dimensional protential source doublet. Actually the microscope slide and coverslip are acting like a Hele Shaw cell (see, for example, Batchelor 1967) with the organism providing the source of momentum. In this case the far field is precisely a two-dimensional potential source doublet with parabolic variation in the strength of the flow field between the plates (Liron & Mochon 1976).

Depending on the size of the organism relative to the size of the container, we can consider the organism as a force concentrated at a point or distributed along a line. This paper will suggest that the flow fields produced by sessile organisms, and in particular the various observed eddies or vortices, are determined primarily by the container geometry in which they are located and not some peculiar property of the organisms' propulsive apparatus.

We discuss here the importance of the following factors in determining the size and the number of eddies;

(i) the zero flux condition;

(ii) confinement due to boundaries in determining the number and shape of eddies;

(iii) the effect of streamline convergence near the force singularities;

(iv) interaction of flow fields from adjacent eddies.

This will be done by considering a series of examples.

In §2 we consider flow fields due to a single stokeslet in various geometries; from a stokeslet parallel to a plane boundary, for which no eddy exists, through to examples such as a stokeslet in an infinite cylinder for which an infinite number of eddies are found to exist. The importance of the zero flux condition and boundary confinement is demonstrated and discussed in detail. In line with the experimental study of Sleigh & Barlow (1976), we consider, in §3, eddy patterns due to a circular distribution of force singularities next to a plane boundary, or between a slide and a coverslip (two parallel plane boundaries). Additional eddies which cannot be explained by the factors (i) and (ii) above are seen. These additional eddies are due to the interaction of the stokeslets. Because of the complicated expressions for the Stokes stream function in these cases, isolating the interaction mechanisms is not straightforward. However, it is much easier to consider the case of two adjacent infinite lines of uniformly distributed stokeslets (two stokeslets in two dimensions) next to a plane boundary which produces qualitatively similar flow fields. This is shown in §4 and is used to explain the existence (or non-existence) and location of the additional eddies, depending on distance between the two lines. All four factors above are now important in determining the eddy structure. A summary of the results and a discussion of the importance of the various factors determining viscous eddy formation is given in the last section, §5.

2. Single stokeslet

An explanation of the existence or otherwise of one or more eddies (infinitely many in some cases) due to the action of a single stokeslet, representing a concentrated directional source of momentum, is presented in this section for a number of specific examples.

(*a*) *Plane boundary*

(i) *Parallel case.* For a stokeslet parallel to a plane boundary no eddy exists. This may be readily seen if one looks at the far-field solution. Consider a stokeslet of unit strength acting at the point $(0, 0, h)$ in the x direction in an (x, y, z) Cartesian co-ordinate system and with the plane boundary located at $z = 0$, then the three components of velocity are given by (Blake 1971)

$$u_i \sim \frac{12hxzr_i}{8\pi\mu r^5} + O\left(\frac{1}{r^3}\right), \quad i = 1, 2, 3, \tag{2.1}$$

where

$$r = |\mathbf{r}|, \quad \mathbf{r} = (r_1, r_2, r_3) = (x, y, z). \tag{2.2}$$

It immediately follows that the velocity in the x direction is always positive. It should be noted that the flux Q created by the above stokeslet in the x direction is proportional to h (Liron 1978). Thus, the boundary, although reducing the flux to a finite value compared to the infinite flux created by a stokeslet in an infinite medium (Liron 1978) is still not sufficient to completely retard the flow and create a vortex or eddy.

(ii) *Normal case.* For a stokeslet located as before but directed normal to the plane boundary, we have axisymmetric flow so we can introduce a Stokes stream function $\psi(r, z)$, where r and z are the radial and axial co-ordinates in cylindrical polar co-ordinates. The stream function is given by Aderogba & Blake (1978). As the flux must be zero in the direction of the force because of the zero (normal) velocity condition on the plane boundary and since there is a positive flow in the normal direction near the stokeslet, there must be a counter-flow further away thus creating an eddy similar to the eddy illustrated later in figure 2(*a*). Only one toroidal eddy exists, extending to infinity both in the radial and axial directions.

(*b*) *Two-dimensional stokeslet near a plane boundary*

The two-dimensional case can be obtained from the three-dimensional solution for a stokeslet by considering an infinite line distribution of three-dimensional stokeslets of uniform strength and direction. The situation here is similar to the previous case with no eddy for a stokeslet parallel to the boundary and two symmetric eddies extending to infinity (instead of one toroidal eddy) for a stokeslet normal to the plane boundary.

Consider a two-dimensional stokeslet of strength $4\pi\mu$ located at $(0, 1)$ (linear dimensions are non-dimensional with respect to the height h of the stokeslet) in an (x, z) Cartesian co-ordinate system and with the plane boundary at $z = 0$. Define a stream function $\psi(x, z)$ with velocities in the x and z directions given respectively by

$$u_x = \frac{\partial\psi}{\partial z}, \quad u_z = -\frac{\partial\psi}{\partial x}. \tag{2.3}$$

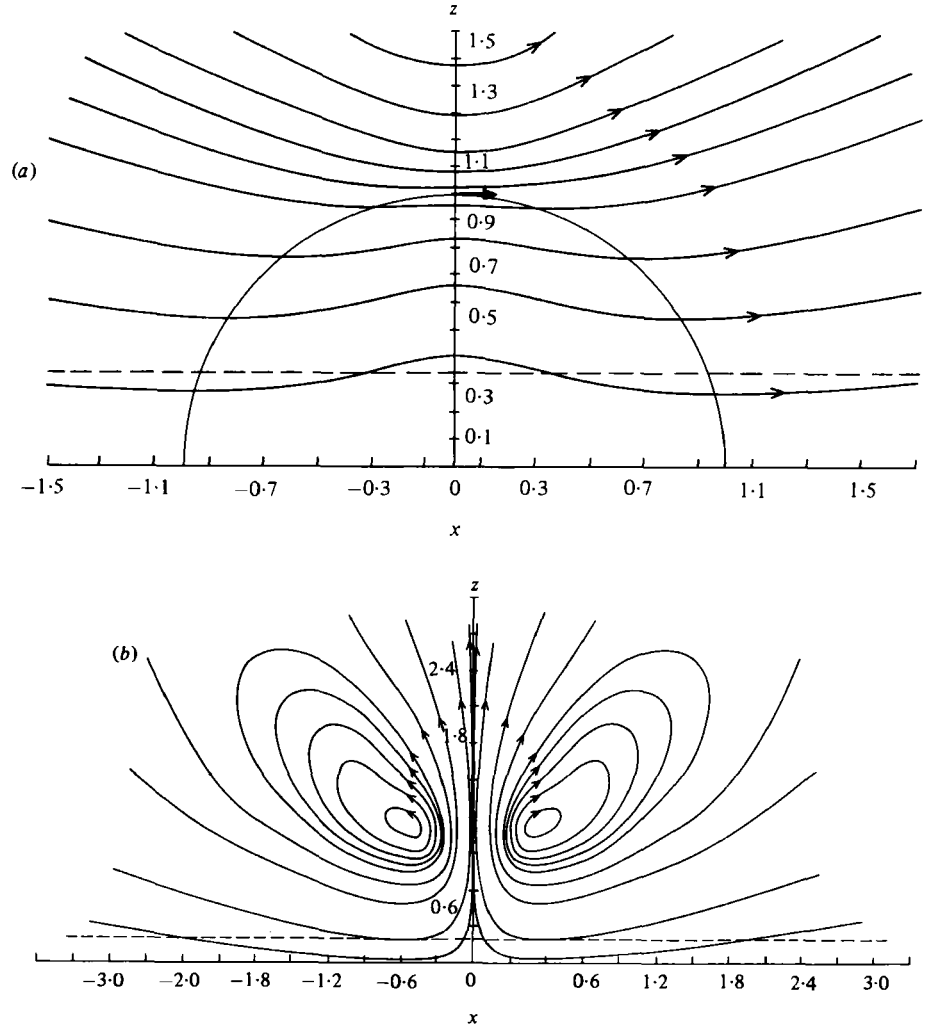

FIGURE 1. Streamlines for a two-dimensional stokeslet above an infinite no-slip plane. (*a*) Stokeslet pointing parallel to the plane boundary, see (2.4). On the circle $x^2+z^2 = 1$ the streamlines are parallel to the plane boundary, $z = 0$. For the dashed line see §4(*b*). (*b*) Stokeslet pointing normal to the plane boundary, see (2.5). Two symmetric infinite eddies now exist. For the dashed line see §4(*a*).

For the stokeslet parallel to the boundary, pointing in the x direction, we obtain

$$\psi(x,z) = \frac{2z(z+1)}{x^2+(z+1)^2} - \tfrac{1}{2}(1-z)\ln\left\{\frac{x^2+(1+z)^2}{x^2+(1-z)^2}\right\}. \tag{2.4}$$

For the stokeslet normal to the boundary, pointing in the z direction, we obtain

$$\psi(x,z) = x\left[\frac{2z}{x^2+(z+1)^2} - \tfrac{1}{2}\ln\left\{\frac{x^2+(1+z)^2}{x^2+(1-z)^2}\right\}\right]. \tag{2.5}$$

The flux in the x direction due to the parallel stokeslet is

$$Q = \psi(x,\infty) = 4, \tag{2.6}$$

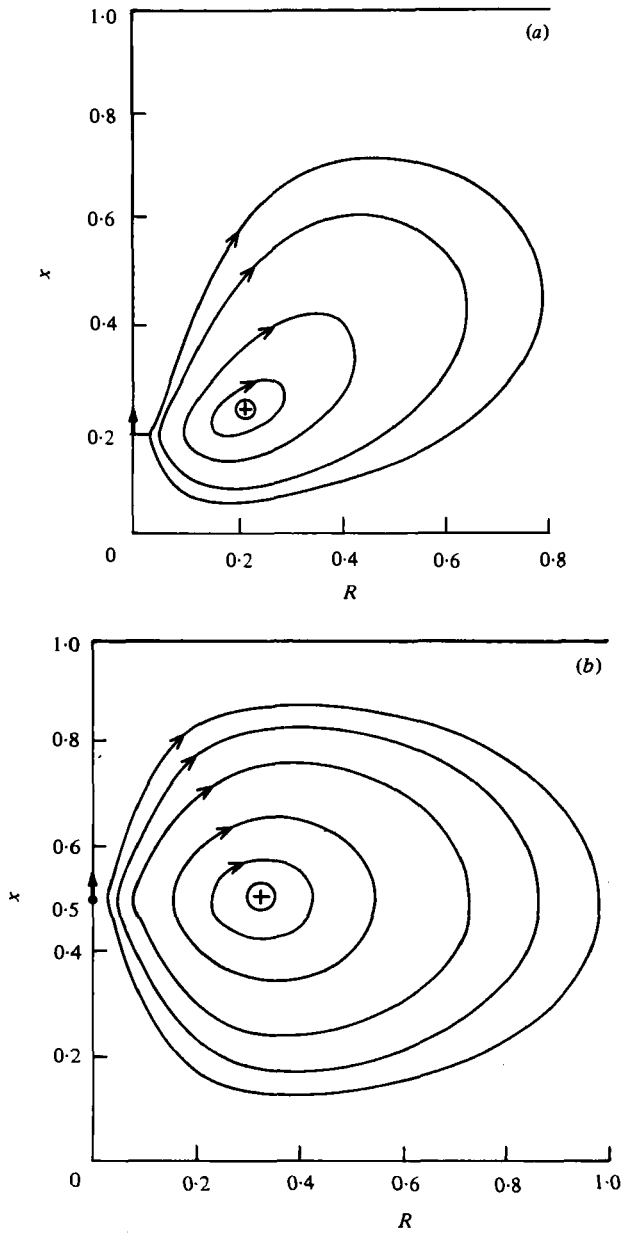

FIGURE 2. The first axisymmetric toroidal (finite) eddy streamlines due to a stokeslet normal to two infinite parallel plane boundaries. (*a*) $h/H = 0{\cdot}2$, (*b*) $h/H = 0{\cdot}5$.

and the flux in the z direction due to the normal stokeslet is obviously zero. Streamlines for the parallel stokeslet are given in figure 1 (*a*) and for the normal case in figure 1 (*b*). These will be used further in § 4 to help to explain stokeslet interactions.

(*c*) *Parallel to, and in between, two plane boundaries*

The solution for a stokeslet between two parallel plane boundaries is given by Liron & Mochon (1976). Although the near field is complicated, the far field rapidly approaches

that of a two-dimensional source doublet in planes parallel to the boundaries with the strength depending parabolically on the distance between the two boundaries. The flux in the direction of the stokeslet is zero (Liron 1978). We thus obtain two circular eddies touching at the origin and extending to infinity, both in the direction of the force and perpendicular to it in planes parallel to the boundaries. Visually, the streamlines appear circular, but particles at different levels would move at different speeds. This is the behaviour one would expect in a Hele Shaw cell.

(*d*) *A stokeslet normal to two plane boundaries*

In this example the flow field will be axisymmetric about the point force so we can use the Stokes stream function $\psi(r,z)$, with radial and axial velocities given respectively by

$$u_r = -\frac{1}{r}\frac{\partial\psi}{\partial z}, \quad u_z = \frac{1}{r}\frac{\partial\psi}{\partial r}. \tag{2.7}$$

For a stokeslet of unit strength located at $r = 0$, $z = h$ the stream function can be obtained by equating the stream-function expression (2.7) for the velocities with equations (47, 48) in Liron & Mochon (1976).

In figure 2(*a*, *b*), graphs of the resulting streamlines are shown for two values of h/H, where H is the distance separating the two plane boundaries. The streamline patterns vary from those approaching the half-space eddies in figure 2(*a*), through to the symmetric eddy illustrated in figure 2(*b*). From the results of a single boundary we would expect to have a toroidal eddy adjacent to the stokeslet. However, it is substantially different from the last case (*c*) in that the axis of eddy rotation is in the azimuthal direction (i.e. parallel to the two boundaries), whereas in the previous case the axis of rotation was normal to the two plates. The existence of only one eddy would imply that it extended to infinity in the radial direction though confined between the plates in the z direction. There is no such solution to the Stokes flow equations at infinity for radial flow which satisfies the no-slip and zero flux conditions, and so it breaks up into an infinite set of eddies with adjacent eddies rotating in the opposite sense, just like the eddies obtained by Moffatt (1964). Solutions of the Stokes flow equations are those exhibiting the least energy dissipation and this is the mechanism used in this case. The eddies become much weaker with distance, decaying exponentially with r. It can be shown that

$$\psi(r,z) \sim A(z,h,H)\, r^{\frac{1}{2}} \exp(-4{\cdot}212r/H)\cos(2{\cdot}251r/H + \delta) \tag{2.8}$$

as $r \to \infty$, where A is an amplitude independent of r, and δ is a phase, also r independent. We thus obtain that the strength of the eddies decay exponentially with r with a wavelength for the eddy structure of

$$\lambda \sim \frac{\pi H}{2{\cdot}251} = 1{\cdot}396H. \tag{2.9}$$

A similar situation occurs in the following example.

(*e*) *Stokeslet in an infinite cylinder*

The solution for this problem was given by Liron (1978) for arbitrary position and orientation and by Blake (1979) for a stokeslet on the axis as well as higher singularities such as a Stokes doublet and a potential source doublet. As in the above case, these

recent studies show the existence of an infinite set of toroidal eddies along the axis of symmetry with a wavelength $\lambda \approx 2{\cdot}15a$, where a is the cylinder radius. The axis of eddy rotation is in the azimuthal direction (i.e. perpendicular to any plane section through the cylinder axis). Thus, again, the eddies cannot expand in the radial direction and consequently break up into an infinite set of exponentially decaying toroidal eddies.

(*f*) *Stokeslet within a finite cylinder*

The introduction of additional boundaries closing the cylinder introduces an additional containment on the fluid. These additional boundaries restrict the number of eddies that can be formed as well as possible changes in shape. Let the height of the cylinder be H, its radius a, and with the stokeslet located on the axis at height h. Blake (1979) has shown the many types of eddies that may exist in such an arrangement. The number, location and shape of the eddies depends on the relative magnitudes of h/H and a/H. If $a/H \gg 1$ (approaching the case (*d*) of two flat plates) then we should obtain a set of eddies in the radial direction, similar to case (*d*), but terminating because of the existence of the outer cylindrical boundary. Likewise, if $a/H \ll 1$ and $h/H = O(1)$ the flow would approach case (*e*) with just a finite number of eddies; the number depending on a/H and the characteristic wavelength given in case (*e*). In addition, near the junction between the cylindrical boundary and the plane boundaries, corner eddies (Moffatt type) will exist, although these are very much smaller than the interior eddies of specific interest to us. Details of this as well as theory and techniques for deriving the expressions for the Stokes stream function in the cylindrical container may be found in Blake (1979) together with illustrations of the shape of the eddies formed.

In summary, the existence of a non-zero flux in the x direction for a force acting parallel to a single plane boundary is disturbing on physical grounds. From momentum considerations the zero flux condition is the obvious constraint as one would not expect a finite force to be capable of moving an infinite volume of fluid. Indeed this may lead to an apparent paradox. For a stokeslet parallel to a plane boundary the flux is non-zero (§§2*a*, 2*b*), but becomes identically zero if an additional parallel plane boundary is placed above the stokeslet; this result being independent of the gap between the boundaries (§2*c*). Of course, where we only have algebraic decay of the velocity, we are usually left with the non-validity of the Stokes flow equations in the far field. Thus, in general, we can only consider these results as being valid in the near field. Exponential decay of the velocities appears to yield a uniformly valid approximation through the entire fluid domain. For example, in the case of a stokeslet normal to two plane boundaries (§2*d*) the velocity decays exponentially to zero by creating an infinite sequence of eddies. As the top plate is displaced to infinity, the primary eddy (adjacent to the stokeslet) expands to fill the entire volume, as can be deduced from (2.9). The solution blends uniformly into that for a stokeslet normal to one plane boundary, which exhibits one infinite three-dimensional toroidal eddy. Here the zero-flux condition holds throughout. For problems which already satisfy the zero-flux condition via exponential decay of velocities, it is seen that the introduction of additional peripheral boundaries, such as closing the cylinder (§2*f*), does not drastically change the flow field, except locally, adjacent to the added boundaries in which corner eddies (Moffatt type) may be introduced and the shape of adjacent eddies distorted.

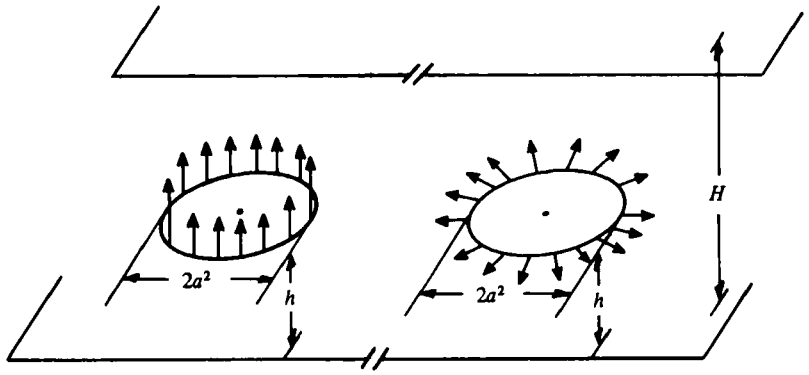

FIGURE 3. Configuration of uniform ring distribution of stokeslets oriented normal to two infinite parallel plane boundaries, and oriented radially, parallel to the boundaries, see §3. For half-space (§3*a*, *b*) we take $H = \infty$.

3. Ring distribution of stokeslets

In this section we look at a ring distribution of stokeslets near a single and two parallel plane boundaries. This would be appropriate when using surface distributions over an axisymmetric body because in this case a ring distribution of stokeslets would be needed. Another example is the previously cited sessile micro-organism *Vorticella* which has a ring of cilia drawing in fluid towards its infundibulum: the cilia in this case are acting as a ring distribution of stokeslets. In separate parts in this section we consider the single plane and the parallel planes examples for the force distribution directed in both the normal and tangential directions.

(*a*) *Single plane boundary, normal orientation*

For a ring distribution of radius a and height h above the plane boundary (see figure 3) an expression can be readily obtained by integrating the radial velocities through 2π and then using (2.7), with x replacing z, to obtain the following expression,

$$\begin{aligned}\psi(r,x) = \frac{1}{\pi}\Bigg[&(r^2-a^2)\left\{\frac{1}{r_2}K(k)-\frac{1}{R_2}K(\kappa)-\frac{2hx}{R_2R_1^2}E(\kappa)\right\}\\&+\left\{r_2E(k)-\frac{(x-h)^2}{r_2}K(k)-R_2E(\kappa)+\frac{(x+h)^2}{R_2}K(\kappa)\right.\\&\left.-2hx\left(\frac{1}{R_2}K(\kappa)-\frac{(x+h)^2E(\kappa)}{R_2R_1^2}\right)\right\}\Bigg],\end{aligned} \tag{3.1}$$

where

$$\begin{aligned}&r_1^2 = (x-h)^2+(r-a)^2, \quad r_2^2 = (x-h)^2+(r+a)^2,\\&R_1^2 = (x+h)^2+(r-a)^2, \quad R_2^2 = (x+h)^2+(r+a)^2,\\&k^2 = 1-\frac{r_1^2}{r_2^2}, \quad \kappa^2 = 1-\frac{R_1^2}{R_2^2}.\end{aligned} \tag{3.2}$$

Here K and E are the complete elliptic integrals of the first and second kind respectively (see Abramowitz & Stegun 1965). Streamline patterns are very similar to those of §4, figure 5(*a–c*). Of particular interest is the opposing finite eddy which lies near

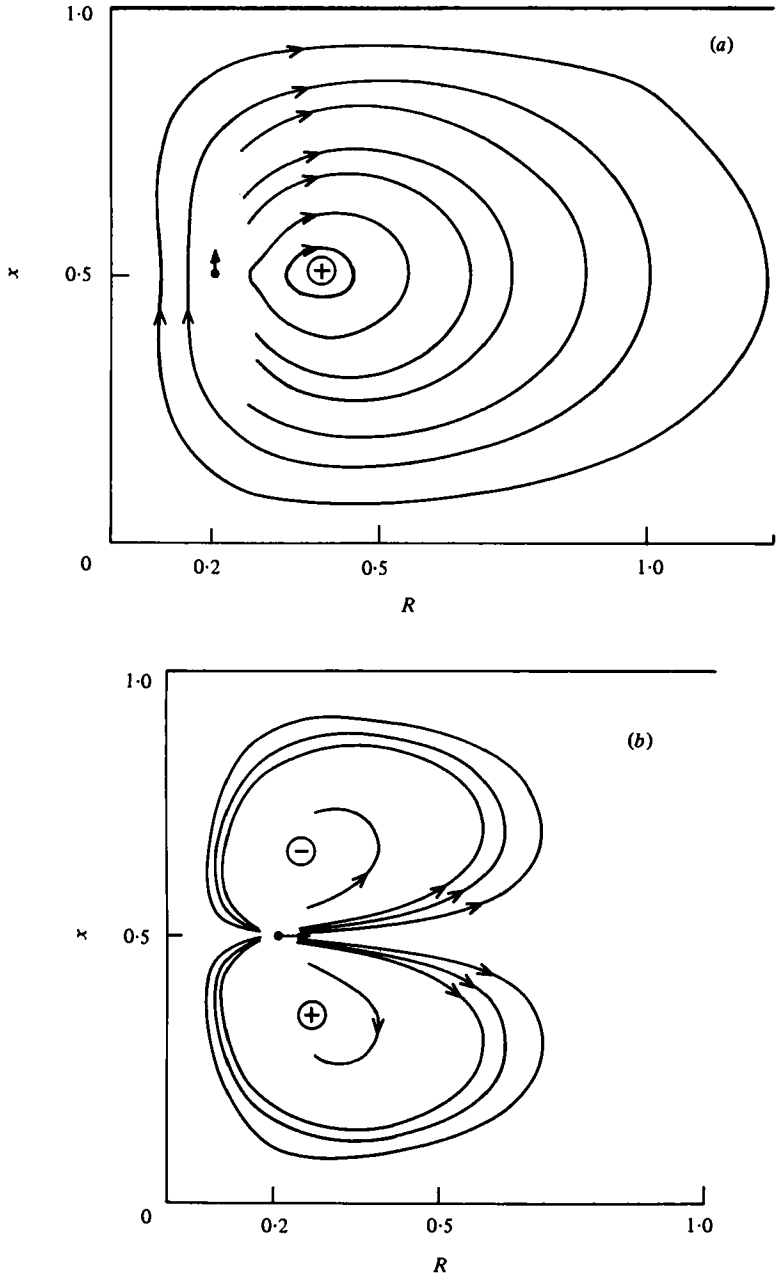

FIGURE 4. Axisymmetric streamlines due to a uniform ring distribution of stokeslets between two infinite parallel plane boundaries, a distance H apart. Ring is at height h and of radius a. (*a*) Vertical orientation $h/H = 0{\cdot}5$, $a/H = 0{\cdot}2$, no internal eddy. (*b*) Radial orientation, $h/H = 0{\cdot}5$, $a/H = 0{\cdot}2$. No internal eddy exists, see (A 3) in the appendix. In both cases an infinite sequence of 'external' toroidal eddies exist, but only the first is shown.

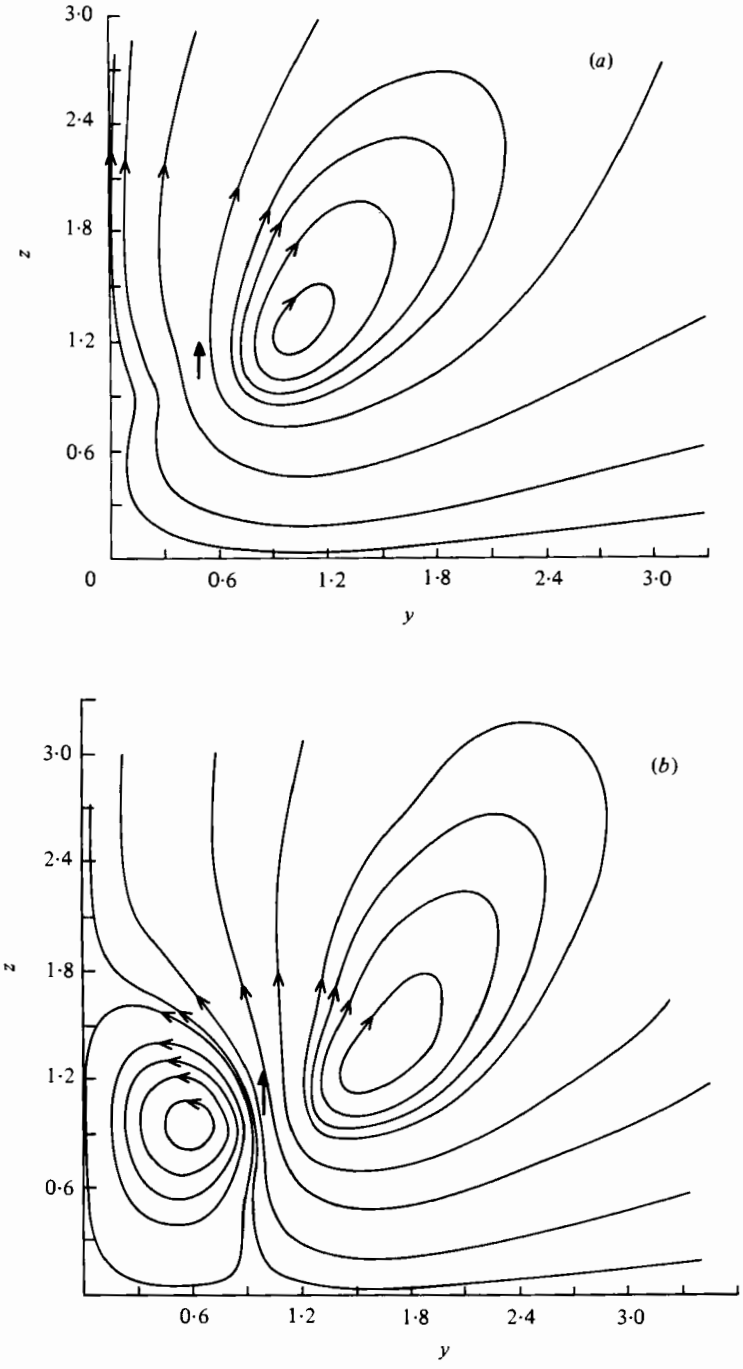

FIGURE 5. Streamlines for a symmetric pair of two-dimensional stokeslets a distance $2a$ apart above a plane boundary. Only the right half-plane is shown. (*a*)–(*c*) Vertical orientation, $a = 0{\cdot}5$, $a = 1{\cdot}0$, $a = 2{\cdot}0$ respectively (see (4.1)), showing results similar to a vertical ring distribution. Internal eddy exists for $a > 1/\sqrt{3}$, see (4.). (*d*)–(*f*) Tangential orientation (the stokeslet at $(-a, 1)$ pointing in the negative y direction), $a = 0{\cdot}5$, $1{\cdot}0$, $1{\cdot}5$ respectively, see (4.2), showing results similar to a radial ring distribution, §3. The internal eddy attaches to the boundary alone as of $a = 1{\cdot}0$, see (4.8).

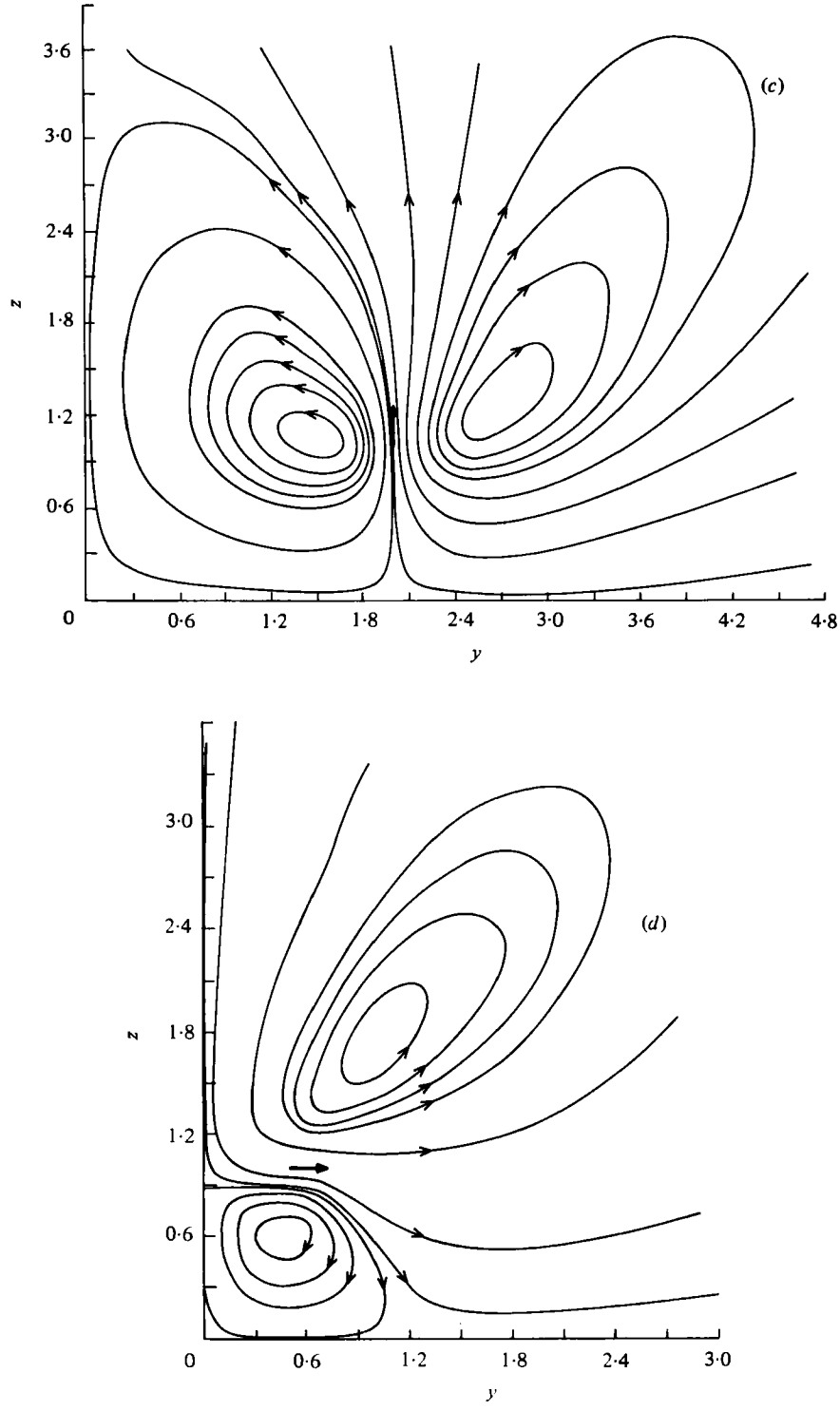

FIGURE 5 (*c*, *d*). For the caption see page 126.

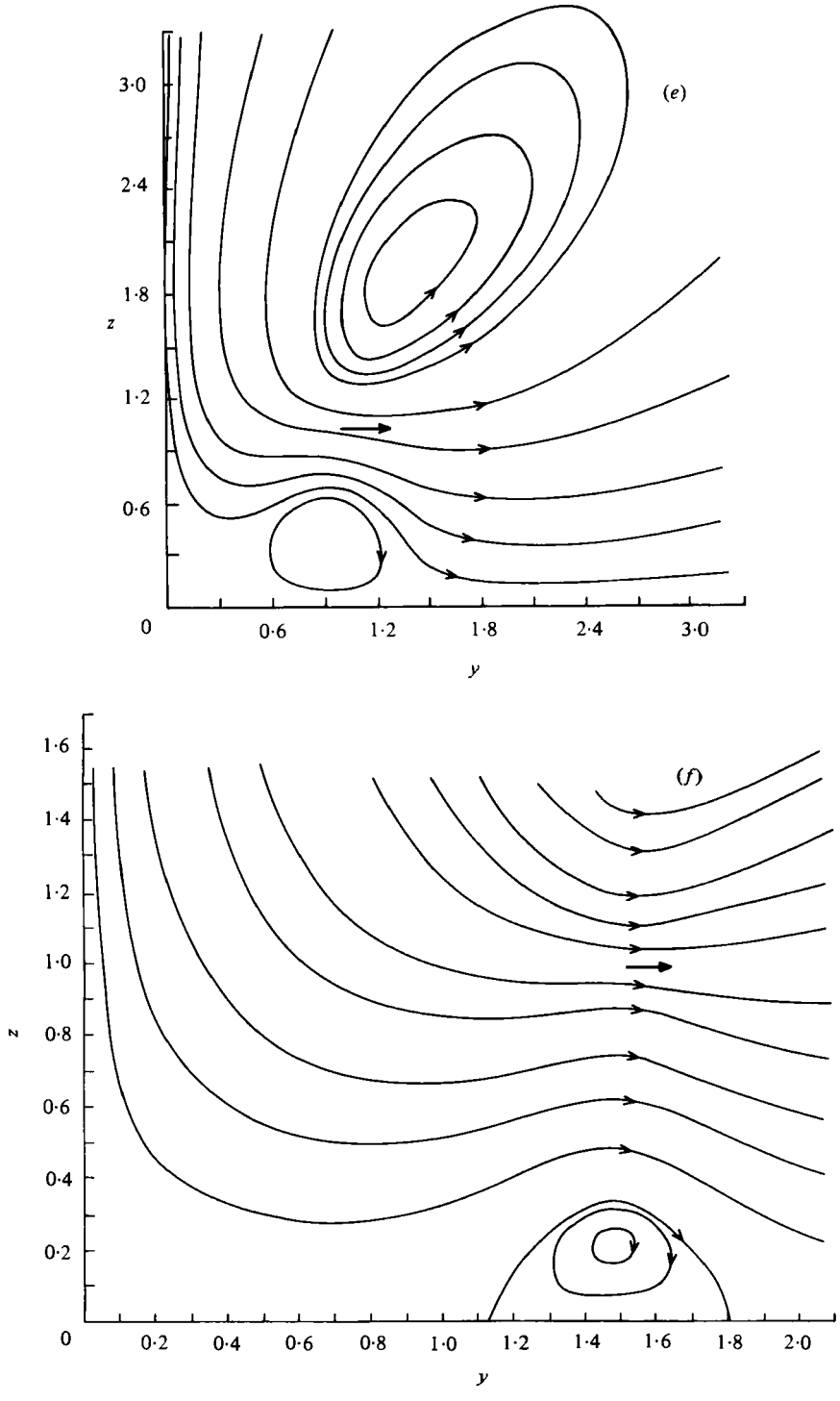

FIGURE 5 (*e*, *f*). For the caption see page 126.

the axis of symmetry adjacent to the rigid boundary that develops when the radius is above a critical value. In the far field the streamlines approach that for the point force example. In the next section a physical explanation of the development of the additional eddies will be given.

(*b*) *Single plane boundary, radial orientation*

In this case no relatively simple expression, as in (3.1), can be easily obtained. However, it is very easy to numerically integrate the following expression to obtain the stream function as a function of position:

$$\frac{\partial \psi}{\partial r} = \frac{1}{\pi}\int_{-1}^{1} r(r\eta - a)\left\{(x-h)\left(\frac{1}{r^3} - \frac{1}{R^3}\right) + \frac{6hx(x+h)}{R^5}\right\}(1-\eta^2)^{-\frac{1}{2}}\,d\eta, \tag{3.3}$$

where

$$r^2 = (x-h)^2 + r^2 + a^2 - 2ar\eta, \quad R^2 = (x+h)^2 + r^2 + a^2 - 2ar\eta. \tag{3.4}$$

Again h is the height of the ring distribution above the plane boundary and a is its radius. Streamline patterns are similar to those in figure 5(*d–f*). An additional eddy always exists. For values of the radius below a critical value, the eddy appears near the axis, but for larger values of radius, a, it is 'trapped' adjacent to the boundary. This too will be explained in § 4.

(*c*) *Two plane parallel boundaries, normal orientation*

In this case we have three important length scales, the 'gap' H between the slide and coverslip, h, the height the distribution is located above the slide, and a, the radius of the ring distribution. The geometry relevant to this problem is shown in figure 3. Obviously as we vary these dimensions the flow fields will change substantially. For example, when h is much less than H, we shall reproduce the results of the half-space fluid above, and if a is much less than both h and H the flow field will approximate the point force solution. Of course in the far field the streamline patterns approach that for a point force with the periodic eddy structure we would expect. An example is given in figure 4(*a*) for $a/H = 0{\cdot}2$, $h/H = 0{\cdot}5$.

(*d*) *Two plane parallel boundaries, radial ring distribution*

The arrangement of the radial ring distribution is illustrated in figure 3. Because of the radial distribution, we have axisymmetry and can use the Stokes stream function in contrast to the point force example. Details on the derivation can be found in the appendix. An example of the resulting streamlines for $a/H = 0{\cdot}2$, $h/H = 0{\cdot}5$ is illustrated in figure 4(*b*). For the cases when the singularities are close to one boundary the single-boundary results of (*b*) are obtained. When the ring distribution is located on the mid-plane an infinite set of pairs of symmetric eddies are obtained.

4. Stokeslet interaction

To explain the interaction of the stokeslets leading to the additional eddies in the last section we shall use a simpler case; that of two parallel lines of uniformly distributed stokeslets (or a pair of two-dimensional stokeslets) near a plane boundary. Let the pair of two-dimensional stokeslets be of strength $4\pi\mu$ situated at $(a, 1)$ and $(-a, 1)$ in a (y, z) Cartesian co-ordinate system with the plane boundary at $z = 0$.

Here we again non-dimensionalize scales with respect to h, the height of the force above the plane boundary. Defining a stream function as in (2.3) with y replacing x, we obtain the stream function for the two two-dimensional stokeslets normal to the plane (i.e. in the z-direction) from (2.5). Thus, we obtain

$$\psi = \frac{4zy[(z+1)^2+y^2-a^2]}{[(y+a)^2+(z+1)^2][(y-a)^2+(z+1)^2]} - \frac{1}{2}\left[(y-a)\ln\left(\frac{(y-a)^2+(z+1)^2}{(y-a)^2+(z-1)^2}\right) + (y+a)\ln\left(\frac{(y+a)^2+(z+1)^2}{(y+a)^2+(z-1)^2}\right)\right]. \quad (4.1)$$

The streamlines of (4.1) for various values of a are illustrated in figure 5 (a–c). As in the last section, we see that the existence or non-existence of an 'internal' eddy depends on the value of a in a fashion qualitatively similar to the ring distribution case.

For the case of two parallel stokeslets with the stokeslet at $(a, 1)$ pointing in the positive y direction and the one at $(-a, 1)$ pointing in the negative y direction, we obtain the stream function from (2.4) as follows,

$$\psi = \frac{8ayz(z+1)}{[(y-a)^2+(z+1)^2][(y+a)^2+(z+1)^2]} + \tfrac{1}{2}(1-z)\ln\left(\frac{[(y+a)^2+(z+1)^2][(y-a)^2+(z-1)^2]}{[(y-a)^2+(z+1)^2][(y+a)^2+(z-1)^2]}\right). \quad (4.2)$$

Streamlines of (4.2) for various values of a are illustrated in figure 5 (d–f). Here we obtain an additional 'internal' eddy either next to the axis of symmetry and boundary or isolated adjacent to the plane boundary; the location depending on the value of a. We use these examples to explain the existence of these additional eddies in the ring distribution examples of the last section. In what follows we shall show that these additional 'internal' eddies derive from the interaction of the two stokeslets and the convergence of streamlines near each of them.

(*a*) *Normal-oriented stokeslets*

The value of the stream function at any point can be obtained by superposing two stokeslet fields as in figure 1 (b), a distance $2a$ apart. When the two stokeslets are far apart ($a \gg 1$) the streamlines in the respective near fields are almost identical with that of the single stokeslet case (2.5), each producing two 'apparently' infinite eddies. Since the two 'inner' eddies are inclined to the axis they will superimpose, cancelling each other's influence in the outer field to produce finite eddies in the inner field. Because of symmetry we have $\psi = 0$ on $y = 0$. Two symmetric closed streamlines between the two stokeslets with a given stream function value are shown schematically in figure 6. As the two stokeslets move closer together these lines pass through positions a–f. As $\psi = 0$ along $y = 0$, the possibility for an eddy closing on the z axis (a separation line $\psi = 0$) is only at a stagnation point (i.e. a point on the axis where $u_z = 0$). Figure 6 (c) shows such a point at the peak (i.e. a turning point where $\partial\psi/\partial y = 0$) of the two eddies and figure 6 (e) shows a similar point at the intersection of the lowest points of these two eddies. Any two such symmetric streamlines will be in one of these positions, and positions c and e cannot be obtained simultaneously (of course for two different stream values). We therefore see that at most there is only one stagnation point z_s on the z axis which moves down as the distance between the two stokeslets decreases.

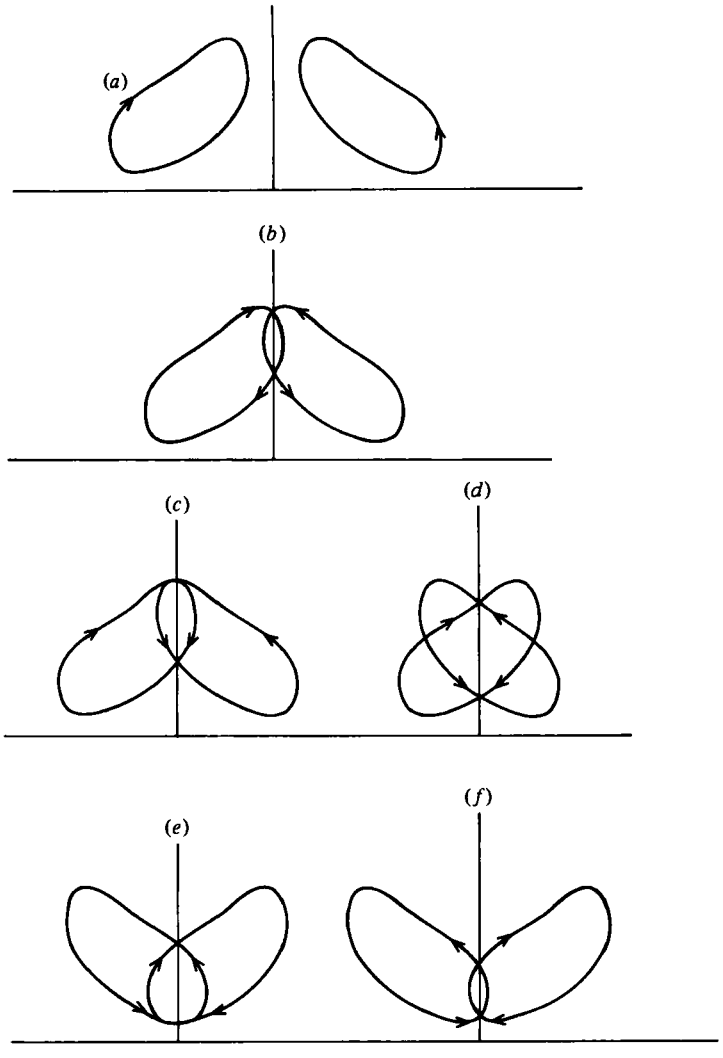

FIGURE 6. Schematic picture of interaction of two symmetric closed streamlines of a pair of two-dimensional stokeslets, oriented normal to a plane boundary. As the two stokeslets move towards each other, the closed streamlines move through positions (*a*)–(*f*). For $a < 1/\sqrt{3}$, see (4.1), all intersecting streamlines will be in position (*f*), and no stagnation point exists on the line of symmetry.

The 'internal eddy', if it exists, must therefore close onto the boundary $z = 0$. Expanding (4.1) for $\psi(y, z)$ near $z = 0$, we obtain

$$\psi \approx -4z^2\left[\frac{y-a}{[1+(y-a)^2]^2}+\frac{a+y}{[1+(y+a)^2]^2}\right]. \tag{4.3}$$

Setting $\psi = 0$ in (4.3), we find that the 'internal' eddy closes on the axis at

$$y_s = [-(a^2+1)+2a(a^2+1)^{\frac{1}{2}}]^{\frac{1}{2}}. \tag{4.4}$$

We find that only one such point exists for $a \geqslant 1/\sqrt{3}$ and none at all for $a < 1/\sqrt{3}$. For $a > 1$ we obtain the following approximation to (4.4) for y_s,

$$y_s \approx a - 1/8a^3, \tag{4.5}$$

which is an accurate approximation as can be seen from figure 5 (*b–c*).

The reason for the existence or non-existence of the 'internal' eddy follows from the behaviour of the stream function in (2.5) near the boundary $z = 0$. Streamlines are drawn towards the stokeslet (see figure 1*b*) and return, circulating below the line $z = 1$. Near $z = 0$ the stream function (2.5) is approximately

$$\psi(x, y) \approx \frac{-4z^2x}{(1+x^2)^2} = 4z^2 f(x). \tag{4.6}$$

For $x < 0$, $f(x)$ is positive with a maximum at $x = -1/\sqrt{3}$, $f(0) = 0$ and $f(x)$ is anti-symmetric. A similar behaviour is seen for $\psi(x, y)$ taken along the dashed line in figure 1 (*b*). This follows because of the circulation of the streamlines. In figure 7 (*a*, *b*) we show the superposition of two such curves, a distance $2a$ apart, for $a < 1/\sqrt{3}$ and $a > 1/\sqrt{3}$. Equation (4.3) is obtained by adding the two. In both cases $\psi < 0$ for $y \geqslant a$ and $\psi = 0$ for $y = 0$. However, in case (*a*) both curves are decreasing, and ψ is negative for all $y \geqslant 0$, whereas in case (*b*) both are increasing so that $\psi > 0$ for $y > 0$ (and y small) and thus there is a point $0 < y_s < a$ such that $\psi = 0$. Moreover from (4.6) we note that the turning point $\partial\psi/\partial x = 0$ near the boundary is at $x = -1/\sqrt{3}$. Thus if $a < 1/\sqrt{3}$ we only have intersections as in figure 6 (*f*) and no stagnation point on the z axis. At $a = 1/\sqrt{3}$ the two stagnation points z_s and y_s collapse onto the point $y = z = 0$ and the 'internal' eddy disappears.

(*b*) *Tangentially oriented stokeslet*

In the case of a single stokeslet oriented parallel to the plane boundary no eddy exists, so we cannot consider the superposition of eddies when considering stokeslet interaction as was the case in part (*a*) of this section. However, the two opposite stokeslets together impose a zero flux condition, thus creating at least one eddy (one toroidal eddy in the axisymmetric case, two eddies in the two-dimensional case because of symmetry about $y = 0$), the 'outer' eddy. The 'internal' eddy, between the two stokeslets, was shown in figure 5 (*d–f*) either to attach to both the boundary ($z = 0$) and axis of symmetry ($y = 0$) or to be isolated near $y = a$, attached only to the boundary. Approximating (4.2) near $z = 0$, we obtain

$$\psi(y, z) \approx 4z^2\left[\frac{(y-a)^2}{[1+(y-a)^2]^2} - \frac{(y+a)^2}{[1+(y+a)^2]^2}\right], \tag{4.7}$$

and thus $\psi = 0$ near $z = 0$ for

$$y_s = [a^2 \pm 1]^{\frac{1}{2}}. \tag{4.8}$$

Approximating (4.2) near $y = 0$, one obtains that $\psi = 0$ near $y = 0$ for

$$z_s = (1-a^2)^{\frac{1}{2}}. \tag{4.9}$$

Thus, if $0 < a \leqslant 1$ we have an eddy connecting the points $(0, (1-a^2)^{\frac{1}{2}})$ and $((1+a^2)^{\frac{1}{2}}, 0)$ while for $a > 1$ there is an eddy attached to the boundary, connecting the points $((a^2-1)^{\frac{1}{2}}, 0)$ and $((a^2+1)^{\frac{1}{2}}, 0)$.

From figure 1 (*a*) we observe that the streamlines of (2.4) are drawn towards the

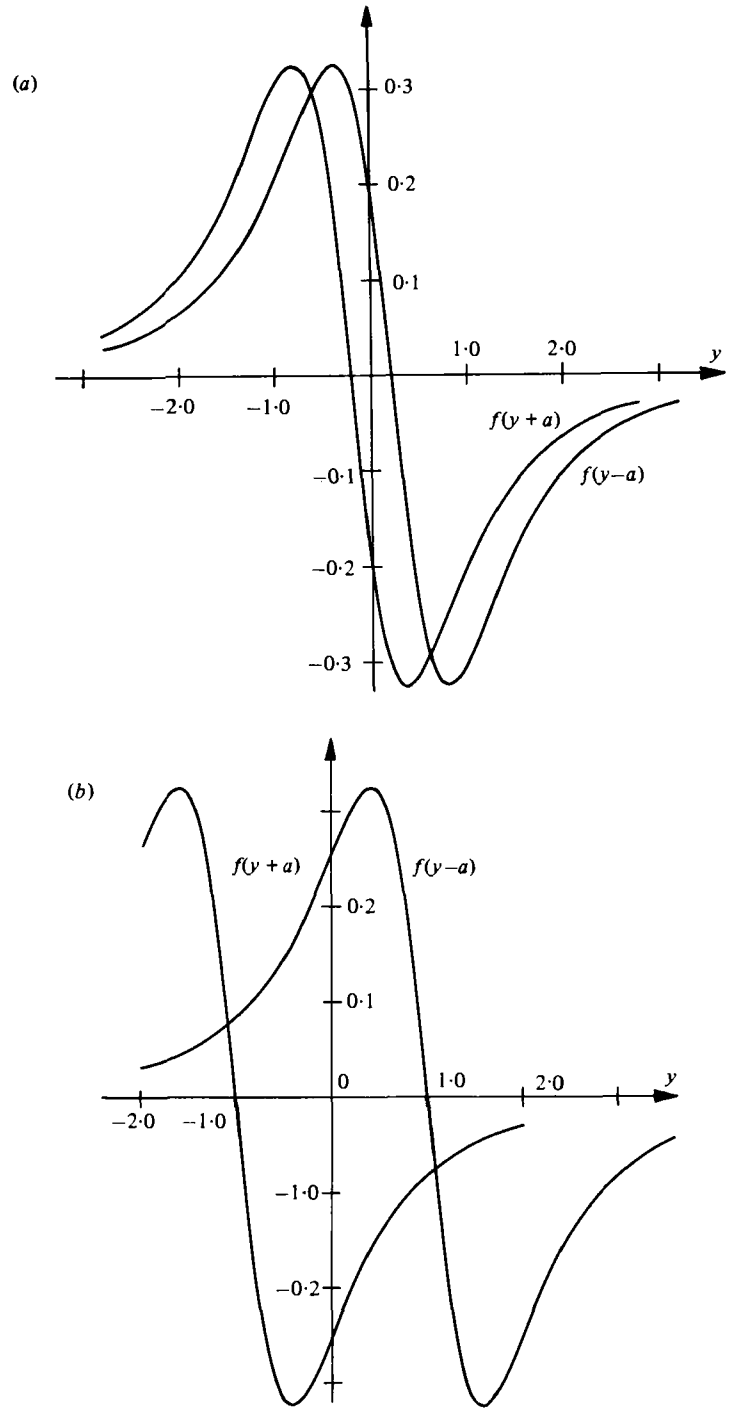

FIGURE 7. Interaction of two stream-function values of a pair of two-dimensional stokeslets a distance $2a$ apart, above a plane boundary. (a)–(b) Normal orientation, for $f(x)$ see (4.6). $a = 0{\cdot}2 < 1/\sqrt{3}$ no internal eddy, $a = 1{\cdot}0 > 1/\sqrt{3}$ internal eddy exists. (c)–(d) Tangential orientation in opposite directions (subtract $g(y+a)$ from $g(y-a)$), for $g(x)$ see (4.10). $a = 1{\cdot}5 > 1{\cdot}0$, eddy attached to boundary only; $a = 0{\cdot}8 < 1{\cdot}0$ internal eddy attached to line of symmetry and boundary.

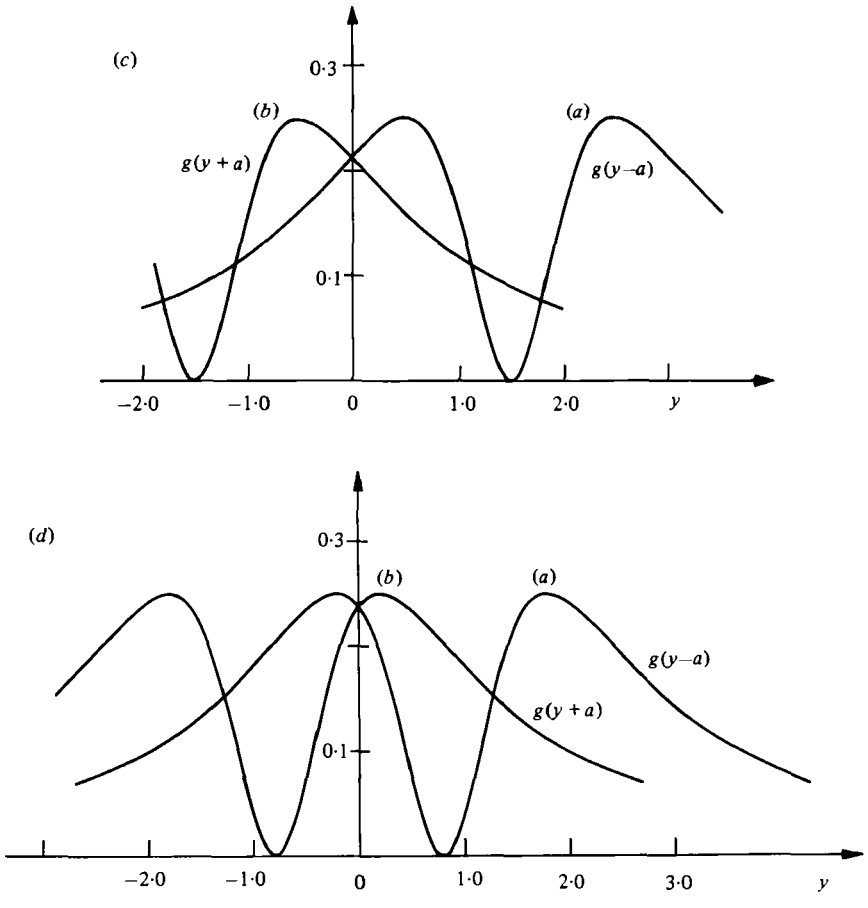

FIGURE 7 (*c*, *d*). For the caption see page 125.

stokeslet at $x = a$, inside the circle $x^2+z^2 = 1$. Thus for each z, $\psi(x, z)$ has a positive local maximum on the circle above and also a local minimum for $x = 0$. Near $z = 0$, we have

$$\psi \approx \frac{4z^2x^2}{(1+x^2)^2} = 4z^2g(x), \tag{4.10}$$

where $g(x)$ is positive and symmetric with a maximum at $x = \pm 1$ and a minimum $g(0) = 0$ at $x = 0$. Consider $\psi(x, z)$ along the dashed line in figure 1 (*a*); we see a similar situation with a maximum at $x = \pm(1-z^2)^{\frac{1}{2}}$ and a minimum at $x = 0$,

$$\psi(0, z) = \frac{2z}{z+1} - (1-z)\ln\left|\frac{1+z}{1-z}\right| > 0, \quad z > 0. \tag{4.11}$$

In figure 7 (*c*, *d*) we show a superposition of two curves $g(y+a)$ and $g(y-a)$ a distance $2a$ apart, for $a > 1$ and $a < 1$. Equation (4.7) is obtained by subtracting curve (*b*) from curve (*a*) in figure 7 (*c*, *d*). Thus where curve (*a*) > curve (*b*) we have $\psi > 0$ and where curve (*a*) < curve (*b*) we have $\psi < 0$. In the case $a > 1$, it is clear that we will obtain two intersections ($\psi = 0$) close to $z = 0$. As z increases $\psi(0, z)$ in (2.4) increases (see (4.11)) and so for a fixed $z > 0$ there will be no intersection of (*a*) (modified with respect

to z) and (b) if a is large enough. Thus, this eddy becomes smaller and smaller as the distance between the two stokeslets increases. For the case $a < 1$ (see figure 7d) it is clear that there is only one intersection of $g(y-a)\,g(y+a)$ for $y > 0$. Therefore there is only one stagnation point for $y > 0$ on the boundary $z = 0$. An increase in z moves the maxima (at $x = \pm(1-z^2)^{\frac{1}{2}}$) closer, which is equivalent to shifting curves (a) and (b) further apart (increasing $2a$) as well as raising the minimum. Thus, at $z_s = (1-a)^{\frac{1}{2}}$ the adjacent maxima of (a) and (b) merge, both $\psi(0, z_s)$ and $\partial\psi(0, z_s)/\partial y$ are zero and the eddy closes on that point.

5. Summary and discussion

In this paper we have investigated the kinematic and dynamic conditions creating one or more viscous eddies due to a single stokeslet or a line of stokeslets near boundaries. The most important condition ensuring the existence of an eddy is the zero-flux condition, such as one obtains when looking at a stokeslet acting normal to a plane boundary. In this case a single (toroidal) eddy extending to infinity, both laterally and in the direction of the force, is obtained. Introducing additional boundaries which prevent the eddy from expanding, obtained for example by adding a plane boundary parallel to the previous one or confining the stokeslet inside an infinite cylinder, results in the breaking up of the single eddy into an infinite sequence of eddies. In this case adjacent eddies rotate in opposite directions and the vorticity decays exponentially in strength away from the stokeslet. Furthermore, due to the exponential decays of the velocity, the Stokes flow equations are uniformly valid throughout the flow domain.

Additional finite eddies appear when we study a ring of stokeslets, for example when modelling the action of a sessile micro-organism between a microscope slide and a coverslip. The existence or non-existence, the shape and location of these additional eddies depend on the radius of the ring relative to its height above the plane boundary. The same results were shown to hold when looking at a pair of two-dimensional stokeslets. This simpler configuration was used to show that the additional eddies are a result of stokeslet interactions combined with the convergence of the streamlines of each stokeslet at its point of action.

As was described in the introduction experiments on sessile micro-organisms show a variety of flow patterns which to date have been unexplained by protozoologists. Our results clearly indicate that these flow patterns are not due to any particular beat of the cilia or flagella of the micro-organism but rather an interaction of the flow field they create with adjacent boundaries. The shape, location and number of eddies generated depend only on the direction of the force produced by the micro-organism, its location and size relative to the boundaries, and the shape of the boundaries.

The major part of this work was carried out at the CSIRO Division of Mathematics and Statistics, Canberra. One of the authors (N.L.) would like to acknowledge the warm hospitality of DMS, CSIRO, where he was an official visitor in July/August 1979. The authors also acknowledge the programming assistance of Andrew Chin.

Appendix. A radially uniform ring of stokeslets parallel to two plane boundaries

The ring of stokeslets is located at $r = a$ and $x = h$, where (x, r) are cylindrical co-ordinates (see figure 3). Let the strength of the stokeslets be $f_0/2\pi a$ per unit length in the radial direction (the total force in any direction being zero). The stream function is

$$\psi = \frac{f_0 H}{4\mu} \operatorname{Im}\left\{ r \sum_{m=1}^{\infty} J_1(\lambda_m a)\, H_1^{(1)}(\lambda_m r)\, a_m(x,h) \right\} \quad \text{for} \quad r > a, \tag{A 1}$$

where λ_m, $m = 1, 2, \ldots$ are the roots in the first quadrant of

$$\sinh^2 \lambda = \lambda \tag{A 2}$$

and the function $a_m(x,h)$ is

$$\begin{aligned} a_m(x,h) = {} & [(1+\lambda_m^2)^{\frac{1}{2}} - 1]^{-1} \{ h x \lambda_m [\sinh \lambda_m (x-h) \\ & + \lambda_m \cosh \lambda_m (x+h) - (1+\lambda_m^2)^{\frac{1}{2}} \sinh \lambda_m (x+h)] \\ & + \lambda_m (x \cosh \lambda_m x \sinh \lambda_m h - h \sinh \lambda_m x \cosh \lambda_m h) \\ & + \sinh \lambda_m h \sinh \lambda_m x [(h-x)(1+\lambda_m^2)^{\frac{1}{2}} + x + h - 1] \}. \end{aligned} \tag{A 3}$$

Here J_1 and H_1^0 are the usual Bessel functions.

In the case $r < a$, interchange the arguments of J_1 and $H_1^{(1)}$. All linear dimensions in (A 1), (A 3) are non-dimensionalized with respect to H.

The derivation of this formula is of interest as it is not straightforward as other cases. By equation (48) of Liron & Mochon (1976), the velocity in the x direction due to a stokeslet at $x = h$, between two plates, and pointing in the α direction ($\alpha = 1, 2$ being the y and z directions respectively) is

$$U_x^{\alpha} = \frac{1}{4H\mu} \frac{\partial}{\partial x_{\alpha}} \operatorname{Im}\left(\sum_{m=1}^{\infty} H_0^{(1)}(\lambda_m \rho)\, a_m(x,h) \right), \tag{A 4}$$

where $a_m(x,h)$ is given in (A 3) and with ρ defined by

$$\rho^2 = a^2 + r^2 - 2ar\cos\phi. \tag{A 5}$$

It follows, from (A 4), that for a force f per unit length in the radial direction, the expression for U_x is

$$U_x = -\frac{f r d\phi}{4H\mu} \frac{\partial}{\partial r} \operatorname{Im}\left(\sum_{m=1}^{\infty} H_0^{(1)}(\lambda_m \rho)\, a_m(x,h) \right), \tag{A 6}$$

and U_x due to the entire ring is found by integrating (A 6) over ϕ from 0 to 2π. Using a formula from Watson (1948), we obtain the following integrated expression for U_x,

$$U_x = \frac{\pi f r}{2\mu H} \operatorname{Im}\left(\sum_{m=1}^{\infty} H_0^{(1)}(\lambda_m r)\, J_1(\lambda_m a)\, \lambda_m\, a_m(x,h) \right), \quad a < r. \tag{A 7}$$

If $f = f_0/2\pi r$, and since $U_x = (1/r)\,\partial\psi/\partial r$, we obtain

$$\psi = \frac{f_0 H r}{4\mu} \operatorname{Im}\left(\sum_{m=1}^{\infty} H_1^{(1)}(\lambda_m r)\, J_1(\lambda_m a)\, a_m(x,h) \right) + f_1(x), \quad a < r. \tag{A 8}$$

Since, for $r \to \infty$, $\psi = 0$, we have $f_1(x) \equiv 0$.

REFERENCES

ABRAMOWITZ, M. A. & STEGUN, I. A. 1965 *Handbook of Mathematical Functions*, pp. 590–592. Dover.

ADEROGBA, K. & BLAKE, J. R. 1978 Action of a force near the planar surface between two semi-infinite immiscible liquids at very low Reynolds numbers. *Bull. Aust. Math. Soc.* **18**, 345–356. Addendum *Bull. Aust. Math Soc.* **19**, 309–318.

BATCHELOR, G. K. 1967 *An Introduction to Fluid Dynamics*, p. 222. Cambridge University Press.

BLAKE, J. R. 1971 A note on the image system for a stokeslet in a no-slip boundary. *Proc. Camb. Phil. Soc.* **70**, 303–310.

BLAKE, J. R. 1979 On the generation of viscous toroidal eddies in a cylinder. *J. Fluid Mech.* **95**, 209–222.

DAVIS, A. M. J. & O'NEILL, M. E. 1977 The development of viscous wakes in a Stokes flow when a particle is near a large particle. *Chem. Engng Sci.* **32**, 899–906.

JEFFREY, D. J. & SHERWOOD, J. D. 1980 Streamline patterns and eddies in low-Reynolds-number flow. *J. Fluid Mech.* **96**, 315–334.

LIRON, N. 1978 Fluid transport by cilia between parallel plates. *J. Fluid Mech.* **86**, 705–726.

LIRON, N. & MOCHON, S. 1976 Stokes flow for a stokeslet between parallel flat plates. *J. Engng Math.* **10**, 287–303.

LIU, C. H. & JOSEPH, D. C. 1978 Stokes flow in conical trenches. *SIAM J. Appl. Math.* **34**, 286–296.

MOFFATT, H. K. 1964 Viscous and resistive eddies near a sharp corner. *J. Fluid Mech.* **18**, 1–18.

SLEIGH, M. A. & BARLOW, D. 1976 Collection of food by *Vorticella*. *Trans. Am. Microsc. Soc.* **95**, 482–486.

WATSON, G. N. 1948 *A Treatise on the Theory of Bessel Functions*, 2nd edn, p. 367. Cambridge University Press.

YOO, J. Y. & JOSEPH, D. C. 1978 Stokes flow in a trench between concentric cylinders. *SIAM J. Appl. Math.* **34**, 247–285.